

UBE3A deletion enhances the efficiency of immunotherapy in non-small-cell lung cancer

Nan Zhang^{a,b}, Jie Shen^a, Lanying Gou^a, Manming Cao^a, Weimin Ding^a, Peng Luo^{a,#}, and Jian Zhang ^{a,#}

^aDepartment of Oncology, Zhujiang Hospital, Southern Medical University, Guangzhou, China; ^bLuoyang Cancer Clinical Diagnosis and treatment Research Center, The Affiliated Luoyang Central Hospital of Zhengzhou University, Luoyang, China

ABSTRACT

Immunotherapy significantly improves the prognosis of advanced lung cancer. It has become an important treatment option for advanced lung cancer. However, there remain many limitations in clinical treatment, and only a small portion of patients can benefit from immunotherapy. Our study aimed to identify markers that can precisely forecast the efficacy of immunotherapy in patients. We analyzed a non-small-cell lung cancer (NSCLC) immune checkpoint inhibitor (ICI) cohort (n=240). We used this discovery cohort to identify CNVs in genes associated with immunotherapy. We further analyzed immune biomarkers and immune infiltration in The Cancer Genome Atlas (TCGA)-NSCLC cohort and the Gene Expression Omnibus (GEO) cohorts. By analyzing an ICI dataset from MSKCC, we found that progression-free survival (PFS) was improved after UBE3A deletion (UBE3A-del). The analysis results showed that UBE3A-del had higher immunocyte infiltration levels and higher expression levels of immune checkpoint biomarkers and affected the enrichment levels of immune signaling pathways. Our results suggest that UBE3A-del can be used as a predictive biomarker of NSCLC to screen for NSCLC patients who may benefit from ICI therapy.

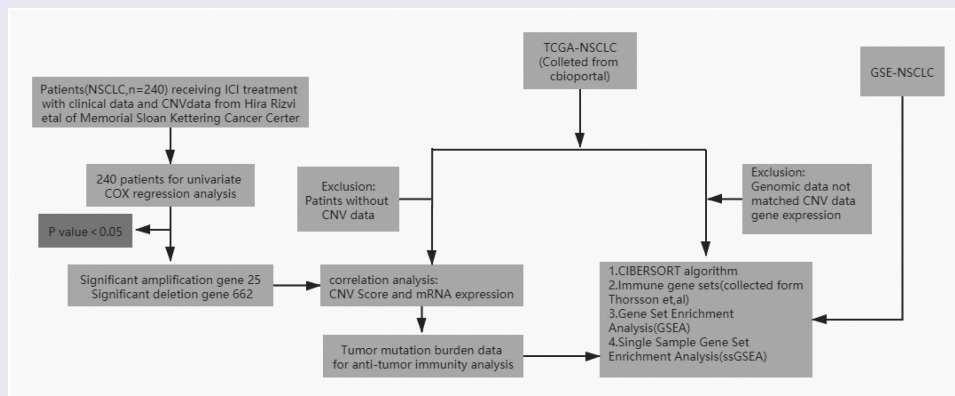
Abbreviations: NSCLC: Non-small cell lung cancer; CNV: Copy number variation; ICIs: Immune checkpoint inhibitors; TCGA: The cancer genome atlas; GEO: Gene expression omnibus; GSEA: Gene set enrichment; PFS: Progression-free survival; OS: Overall survival; TMB: Tumor mutational burden; CTLA-4: Cytotoxic T lymphocyte antigen 4; PD-(L)1: Programmed cell death (ligand) 1; MSI: Microsatellite instability; dMMR: DNA mismatch repair; SCNAs: Somatic copy number alterations; TME: Tumor microenvironment; MSK-IMPACT: The Memorial Sloan Kettering-Integrated Mutation Profiling of Actionable; Cancer Targets; FDA: Food and Drug Administration; WES: Whole-exome sequencing; SNP: Single Nucleotide Polymorphisms; FDR: False discovery rate; DCR: Disease control rate; DDR: DNA damage response and repair; MDSCs: Myeloid-derived suppressor cells; FAO: Fatty acid oxidation





ARTICLE HISTORY

Received 25 February 2022
Revised 14 April 2022
Accepted 18 April 2022


KEYWORDS

Immune checkpoint inhibitors; biomarker; non-small-cell lung cancer (NSCLC); UBE3A; deletion



CONTACT Peng Luo  luopeng@smu.edu.cn  Department of Oncology, Zhujiang Hospital, Southern Medical University, Guangzhou, China; Jian Zhang  blacktiger@139.com  Department of Oncology Zhujiang Hospital, Southern Medical University, Luoyang, China

[#]The two correspondence authors have contributed equally.

 Supplemental data for this article can be accessed online at <https://doi.org/10.1080/21655979.2022.2069328>

© 2022 The Author(s). Published by Informa UK Limited, trading as Taylor & Francis Group.

This is an Open Access article distributed under the terms of the Creative Commons Attribution License (<http://creativecommons.org/licenses/by/4.0/>), which permits unrestricted use, distribution, and reproduction in any medium, provided the original work is properly cited.

Highlights

- Our topic is interesting and investigates a current and concrete unmet clinical need, given the lack of reliable predictors of benefit for immunotherapy in NSCLC. We first identified *UBE3A*-del as a biomarker of immunotherapy response from an ICI-treated cohort (the MSKCC dataset).
- We found that PFS of patients was improved after *UBE3A* deletion in ICI-treated cohort. To investigate the relationship of *UBE3A*-del and immunotherapy, we verified it in the non ICI-treated cohorts, a TCGA dataset and two GEO datasets. After analysis, we determined that *UBE3A*-del has a close relationship to the efficacy of immunotherapy. *UBE3A*-del showed higher TMB in the ICI dataset and TCGA-NSCLC dataset. *UBE3A*-del showed a better disease control rate (DCR).
- Difference analysis of TCGA transcriptome data showed that *UBE3A*-del mRNA expression was lower and that the CNV fraction was positively correlated with RNA expression, *UBE3A*-del methylation degree was higher, expression of some proteins was higher after *UBE3A*-del.
- *UBE3A*-del enhances immune infiltration. Our results showed that immune genes, immune cells, chemokines and immune checkpoint markers were significantly upregulated in *UBE3A*-del. Our results show that *UBE3A*-del enhances antitumor immunity and immunogenicity.
- *UBE3A*-del is enriched in the immune pathway. Our results showed that *UBE3A*-del

activated the DNA damage repair mismatch complex pathway and immune pathway.

Introduction

Background

The rise of tumor immunotherapy is setting off a new revolution in tumor treatment. Compared with the traditional curative effect, the lasting curative effect is an important advantage of immunotherapy. Immunotherapy has made rapid progress in lung cancer, bringing new hope for advanced lung cancer and becoming an important treatment for advanced lung cancer. However, only a few people show sustained responses, and we need to search for effective biomarkers that can identify potential beneficiaries [1–4].

Previous studies have shown that PD-L1 expression, tumor mutational burden (TMB), microsatellite instability (MSI), deficient DNA mismatch repair (dMMR), immune microenvironment (CD8 + T cell and immune factors), and neoantigen load can predict the response of various tumor types to ICIs [5–13]. However, these predictors have some limitations, and the detection methods and evaluation criteria have not been unified. Therefore, the detection of gene mutations has higher specificity in guiding immunotherapy.

Previous studies have mostly followed the effects of somatic mutations on immunotherapy [14–17]. In the near future, it has been reported that copy number variation is closely related to immunotherapy. Aneuploidy, also known as SCNAs, is considered to

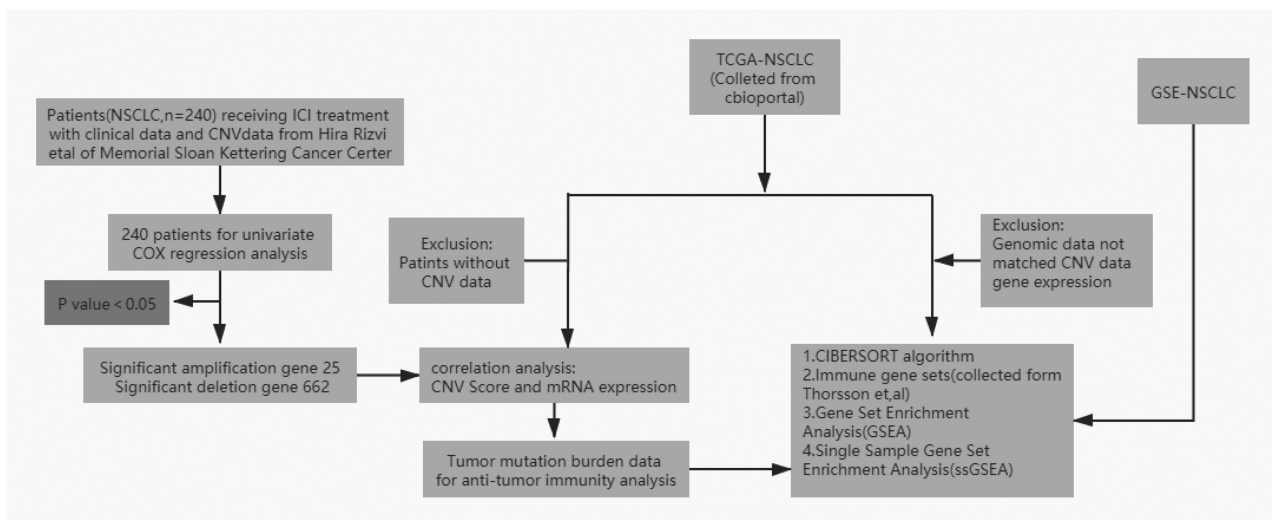


Figure 1. Analysis flow chart.

be one of the factors leading to tumor development. Teresa Davoli et al. found that the SCNA level could predict markers of cytotoxic immunocyte infiltration better than TMB by exploring a clinical cohort of immunotherapy in patients with melanoma [18,19]. Therefore, SCNA can be used to guide clinical treatment.

In this study, CNV and clinical information from multiple databases were collected to identify gene CNVs associated with ICI efficacy. We found that *UBE3A* gene deletion (*UBE3A*-del) showed higher TMB and better PFS, and CNV level of *UBE3A* was correlated with mRNA, methylation and proteomics. After *UBE3A* gene deletion, a better curative effect was achieved by increasing immunocyte infiltration and activating immune pathways [Figure 1].

Methods

Clinical cohort

To assess the influence of SCNA on the curative effect of ICIs, we analyzed a discovery cohort. From HIRA Rizvi et al. (<https://www.cbiportal.org>), a dataset of 240 non-small-cell lung cancer patients was used. MSK-impact sequencing was used in our study, an entire genomic analysis panel authorized for use by the Food and Drug Administration (FDA) [20].

We further analyzed the immune biomarkers and immune infiltration in TCGA-NSCLC, and 586 patients with NSCLC were collected from the TCGA dataset (<https://www.cbiportal.org>) [21], mainly including whole-exome sequencing (WES), chromosome CNV, transcriptome, methylation, protein chip and clinical data. In addition, Gene Expression Omnibus (GEO) datasets (GSE43580 and GSE63074) containing gene expression data were used to verify the results by analyzing the GEO transcriptome data.

CNV analysis

We used GISTIC 2.0 to analyze the arm-level SCNA of copy number [22]. For TCGA data, CNVs were measured by the Affymetrix SNP 6.0 chip, the original data were processed by picnic software to obtain

the segment file, and usually, the SEG of diploid was zero. Mean values of -0.2 and 0.2 were used to determine whether the region was deleted or amplified. Based on the G score and Q value, CNVs with significant variation were identified. False discovery rate (FDR) values exceeding the level ($Q < 0.25$) were significant. The results of GISTIC 2.0 were shown by the R package maftools [23].

Analysis of tumor immunogenicity

The CIBERSORTx deconvolution method was used to estimate the levels of tumor immunocyte infiltration [24]; 22 types of immunocyte infiltration levels in *UBE3A*-del and *UBE3A*-wt were compared, and the outcomes were visualized by the R package ggpubr.

Pathway enrichment analysis

We used edgeR to analyze the transcriptome data of the TCGA-NSCLC and GEO cohorts. Then, we used clusterProfiler to analyze the correlation of CNVs and the activation levels of pathways [25,26]. The gene expression of the TCGA-NSCLC and GEO cohorts was analyzed by single-sample gene set enrichment analysis (ssGSEA) with GSVA. Finally, we used the R package pheatmap to visualize the results.

Statistical analysis

We used the Mann–Whitney U test to analyze TMB discrepancies, mRNA expression, methylation values, immunocyte infiltration levels and immune checkpoint biomarkers from *UBE3A*-del. Kaplan–Meier survival analysis and Cox regression analysis were used to analyze the PFS and OS of *UBE3A*-del and *UBE3A*-wt. We used the R package ggstatplot to estimate the relationship between CNV status and mRNA and methylation in the TCGA dataset. The limma R package was used to analyze the protein chip expression of *UBE3A*-del and *UBE3A*-wt in the TCGA dataset [27]. We used the edgeR package to analyze the differences in immune genes. The significance level was 0.05, and all

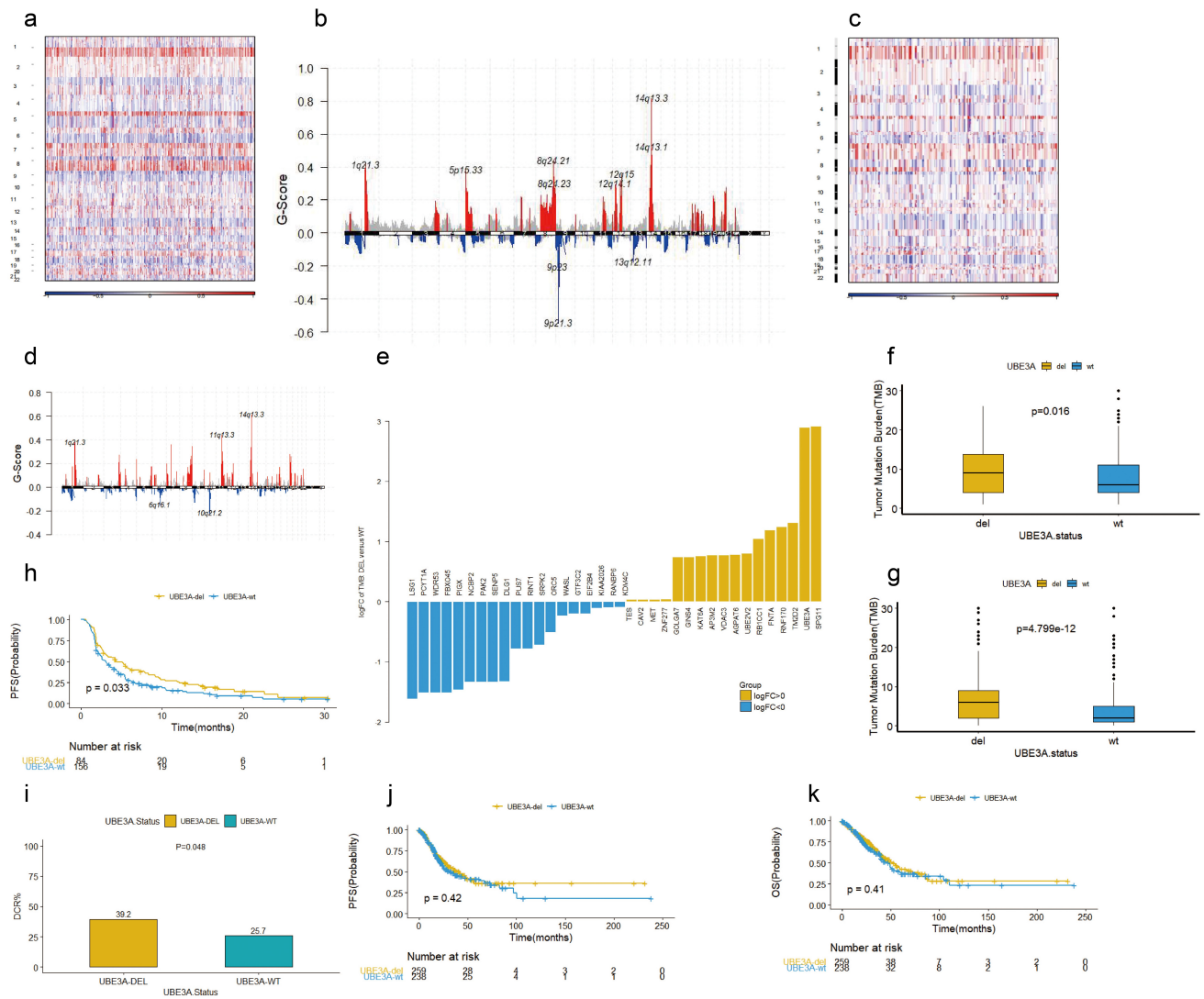


Figure 2. The predictive value of *UBE3A*-del for NSCLC ICI treatment. (a) Results of CNV GISTIC analysis of the TCGA-NSCLC non-ICI cohort: Overview of the chromosomal changes. (b) Comparison of significantly amplified and deleted chromosomes (TCGA). Red represents significantly amplified chromosomes, and blue represents significantly deleted chromosomes. (c) Results of CNV GISTIC analysis of the MSKCC NSCLC ICI cohort: Overview of the chromosomal changes. (d) Comparison of significantly amplified and deleted chromosomes (MSKCC). Red represents significantly amplified chromosomes, and blue represents significantly deleted chromosomes. (e) Relationship between CNV and TMB in the non-ICI cohort of TCGA-NSCLC: Difference between deletion or amplification of the CNV gene and wild-type TMB. (f) Comparison of *UBE3A*-del and *UBE3A*-wt TMB in the NSCLC ICI cohort. (g) Comparison of *UBE3A*-del and *UBE3A*-wt TMB in the NSCLC non-ICI cohort. (h) Survival analysis of PFS in the NSCLC ICI dataset between *UBE3A*-del and *UBE3A*-wt. (i) Comparison of the disease control rate (DCR) between *UBE3A*-del and *UBE3A*-wt in the NSCLC ICI cohort. (j) Survival analysis of PFS in the NSCLC non-ICI dataset between *UBE3A*-del and *UBE3A*-wt. (k) Survival analysis of OS in the NSCLC non-ICI dataset between *UBE3A*-del and *UBE3A*-wt.

statistical tests were two-sided. Statistical analysis was completed using R v.3.6.1.

Results

UBE3A-del increases the efficacy of immunotherapy

We performed GISTIC analysis on 586 NSCLC samples from the TCGA cohort (Figure 2(a,b)).

The results showed that some chromosomes were significantly amplified ($Q < 0.25$, Fig. S1A), such as 14q13.3, 1q21.3, 12q15, 5p15.33, and 8q24.21. Some chromosomes were significantly deleted ($Q < 0.25$, Fig. S1B), such as 9p21.3, 9p23, 13q12.11, and 22q13.32. We verified the results of the ICI cohort according to the GISTIC analysis results (Figure 2(c,d)). GISTIC analysis of 240 NSCLC patients from HIRA Rizvi et al. showed

that some chromosomes were significantly amplified ($Q < 0.25$, Fig S1C), such as 14q13.3, 1q21.3, 7p11.2, 8q24.3, and 5p15.33, and some chromosomes were significantly deleted ($Q < 0.25$, Fig. S1D). Through the next analysis, genes with significant amplification and significant deletion of chromosomal sites, which were significantly related to SCNA, were found.

We further explored the relationship between CNV and prognosis in 240 NSCLC patients treated with ICIs including available CNV and clinical data from HIRA Rizvi et al. [28]. According to the

status of CNVs (deletion or amplification), genes corresponding to significant deletions or amplified chromosomes were included (GISTIC analysis results). Univariate regression analysis was used to analyze the PFS of ICI efficacy. The results showed that 25 genes were significantly amplified ($P < 0.05$), such as *ABCG1*, and 662 genes were significantly deleted ($P < 0.05$), such as *UBE3A*. Then, the genes with significant amplification and deletion were verified in the TCGA cohort. According to the CNV amplification or deletion score and RNA expression in the TCGA cohort,

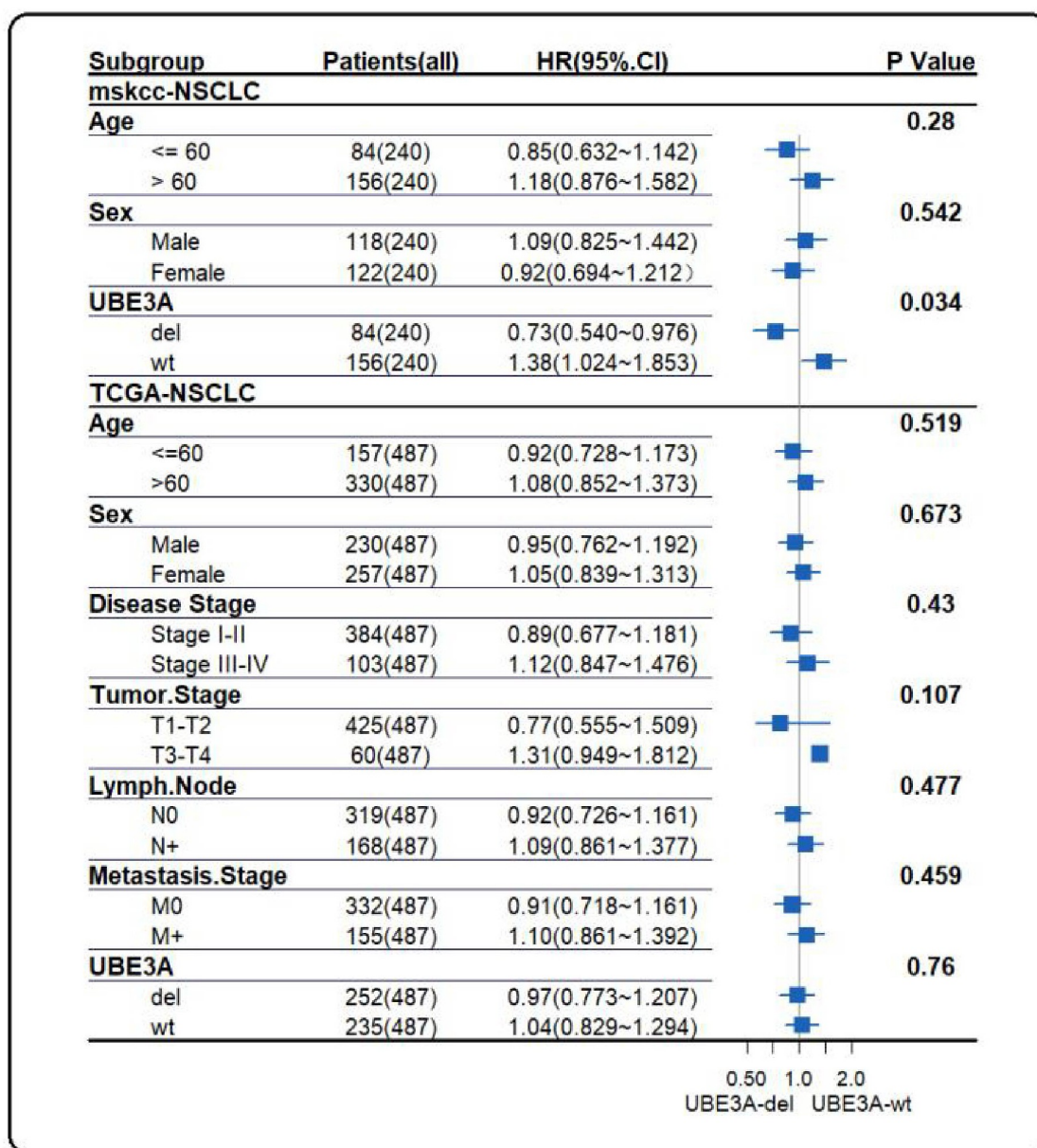


Figure 3. Hierarchical analysis of the MSKCC cohort and TCGA cohort. Age, sex, stage and *UBE3A* CNV status of the MSKCC cohort and TCGA cohort were analyzed.

a total of 36 genes with correlation coefficients > 0.6 were all significantly deleted genes, such as *UBE3A* and *SPG11*. After analysis, we determined that *UBE3A*-del has a close relationship to the efficacy of immunotherapy. *UBE3A*-del showed higher TMB in the ICI dataset and TCGA-NSCLC dataset (Figure 2(e), $p = 0.016$, Figure 2(f); $p = 2.825e-12$, Figure 2(g)).

***UBE3A*-del and clinical outcomes**

In the MSKCC cohort of HIRA Rizvi et al. 84 cases were *UBE3A*-del, and 156 cases were *UBE3A*-wt. All patients were treated with single or combined immune checkpoint inhibitors. Survival analysis showed that *UBE3A*-del prolonged PFS ($P = 0.033$, Figure 2(h)), and *UBE3A*-del showed a better disease control rate (DCR) ($P = 0.048$, Figure 2(i)). The expression of PD-L1 was not significantly different between the two groups ($P = 0.96$, Fig. S1E).

There were 506 cases of CNV sequencing in the TCGA cohort. According to the status of CNV, 264 cases were *UBE3A*-del, and 242 cases were *UBE3A*-wt. Survival analysis showed that PFS was not significantly different in the TCGA-NSCLC dataset ($P = 0.42$, Figure 2(j)). Similarly, there was no OS benefit ($P = 0.41$, Figure 2(k)). Hierarchical analysis of the MSKCC dataset and TCGA dataset was consistent in the age, sex, and stage subgroups (Figure 3, all cases > 0.05). This finding suggests that the improvement in PFS in *UBE3A*-del patients in the MSKCC cohort may be caused by immunotherapy.

Correlation between the CNV status of the *UBE3A* gene and RNA, methylation, and protein levels

Difference analysis of TCGA transcriptome data showed that *UBE3A*-del mRNA expression was lower ($P < 2.2e-16$, Figure 4(a)) and that the CNV fraction was positively correlated with RNA expression ($P < 0.001$, Pearson = 0.61, Figure 4(b)). This finding was consistent with that of a previous report, which was also verified later in the GEO cohort [29]. We analyzed the common driver genes of NSCLC and found that the mRNA expression of *BRAF*, *KRAS* and *MET* was higher after *UBE3A*-del ($P < 2.2e-16$, Figure 4(c)), which suggested that *UBE3A*-del patients might be

sensitive to targeted therapy, which was in accordance with previous research from Mazieres et al. They revealed that the ICI response rate of lung cancer driven by *KRAS*, *BRAF* and *MET* was higher than that of other driver genes [30]. The difference analysis of the methylation beta value showed that the *UBE3A*-del methylation degree was higher ($P = 1.216e-05$, Figure 4(d)), and there was a negative correlation between the two groups ($P = 0.018$, Pearson = -0.11 , Figure 4(e)), which was in accordance with the research of Hyunchul Jung et al. [31]; genomic methylation changes offset the influence of TMB and reduce the effect of immunotherapy.

Finally, by analyzing the protein chip data of TCGA-NSCLC, it was found that the expression of some proteins was higher after *UBE3A*-del ($P < 0.05$, Figure 4(f)). For example, *MAPK* and *NOTCH1*, in our study, the expression of these proteins in *UBE3A*-del exceeded that in *UBE3A*-wt [32,33].

***UBE3A*-del enhances immune infiltration**

To research the influence of *UBE3A*-del on immune infiltration, CIBERSORTx was used to analyze the immunocyte infiltration abundance of the TCGA-NSCLC cohort. We discovered that the infiltration degree of M1 macrophages, M0 macrophages, and activated mast cells was increased in *UBE3A*-del ($P < 0.05$, Figure 5(a)). We further analyzed the immune infiltration of *UBE3A*-del in the TCGA-NSCLC dataset. The results showed that immune genes, such as *AHSA1*, *ADRM1*, and *CCT5*, which activated CD8 cells, and *CASC5*, *CCNB1*, and *CCNE2*, which activated CD4 cells, were enriched in *UBE3A*-del ($P < 0.05$, Figure 5(b))[34]. Moreover, chemokines (*CXCL10* and *CXCL9*) and immune checkpoint markers (*TIGIT*, *PDCD1* and *LAG3*) were significantly upregulated in *UBE3A*-del ($P < 0.05$, Figure 5(c)).

Next, we verified the immune cell infiltration abundance of the GSE43580 and GSE63074 datasets in the GEO cohort by CIBERSORTx. On the basis of the median mRNA expression, we obtained two groups: *UBE3A*-high and *UBE3A*-low. Memory cells, B cells and M1 macrophages were enriched in *UBE3A*-low cells ($P < 0.05$, Figure 5(d,e)). Some immune-related genes, such as *GPR183*, *SLFN11*, *ZEB2*, *CD2*, and *CD27*, which activate CD8 T cells, and *MAL*, *CCL5*, and *CXCR6*, which activate CD4 T cells, were significantly upregulated in *UBE3A*-low cells ($P < 0.05$, Figure 6(a,b)). The expression of cytokines (*CCL5*,

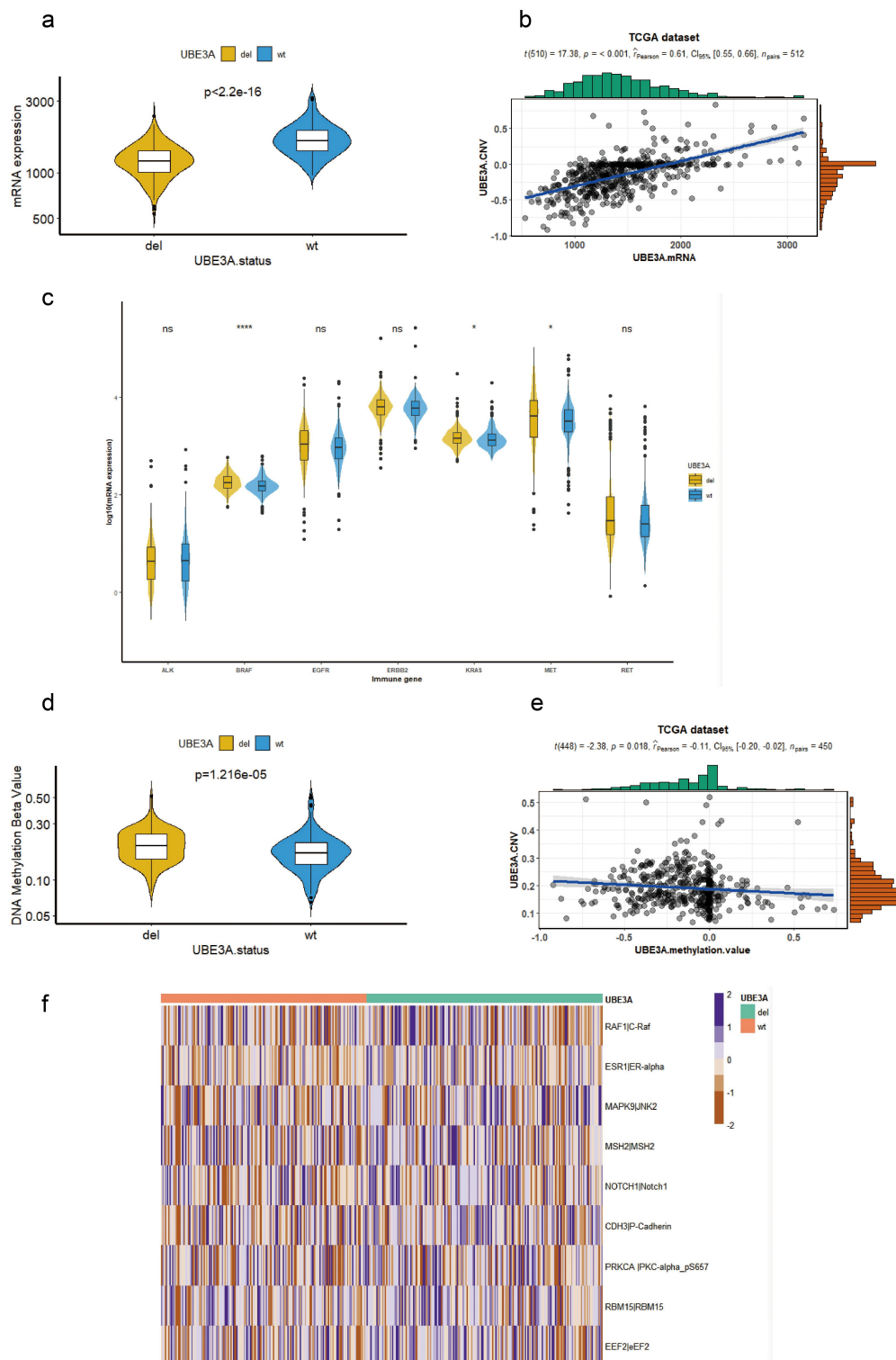


Figure 4. CNV status of the *UBE3A* gene at the RNA, methylation and protein levels and correlation analysis. (a) Difference in the mRNA expression of *UBE3A*-del and *UBE3A*-wt in the TCGA dataset. (b) The relationship between the *UBE3A* CNV fraction and *UBE3A* mRNA expression was analyzed. (c) Differences in common driver genes between *UBE3A*-del and *UBE3A*-wt in the NSCLC dataset. (d) Different degrees of methylation between *UBE3A*-del and *UBE3A*-wt in the NSCLC cohort. (e) The relationship between the *UBE3A* CNV score and the *UBE3A* methylation beta value. (f) Heatmap display of differences in *UBE3A*-del and *UBE3A*-wt protein expression in the NSCLC cohort. Each line represents a protein.

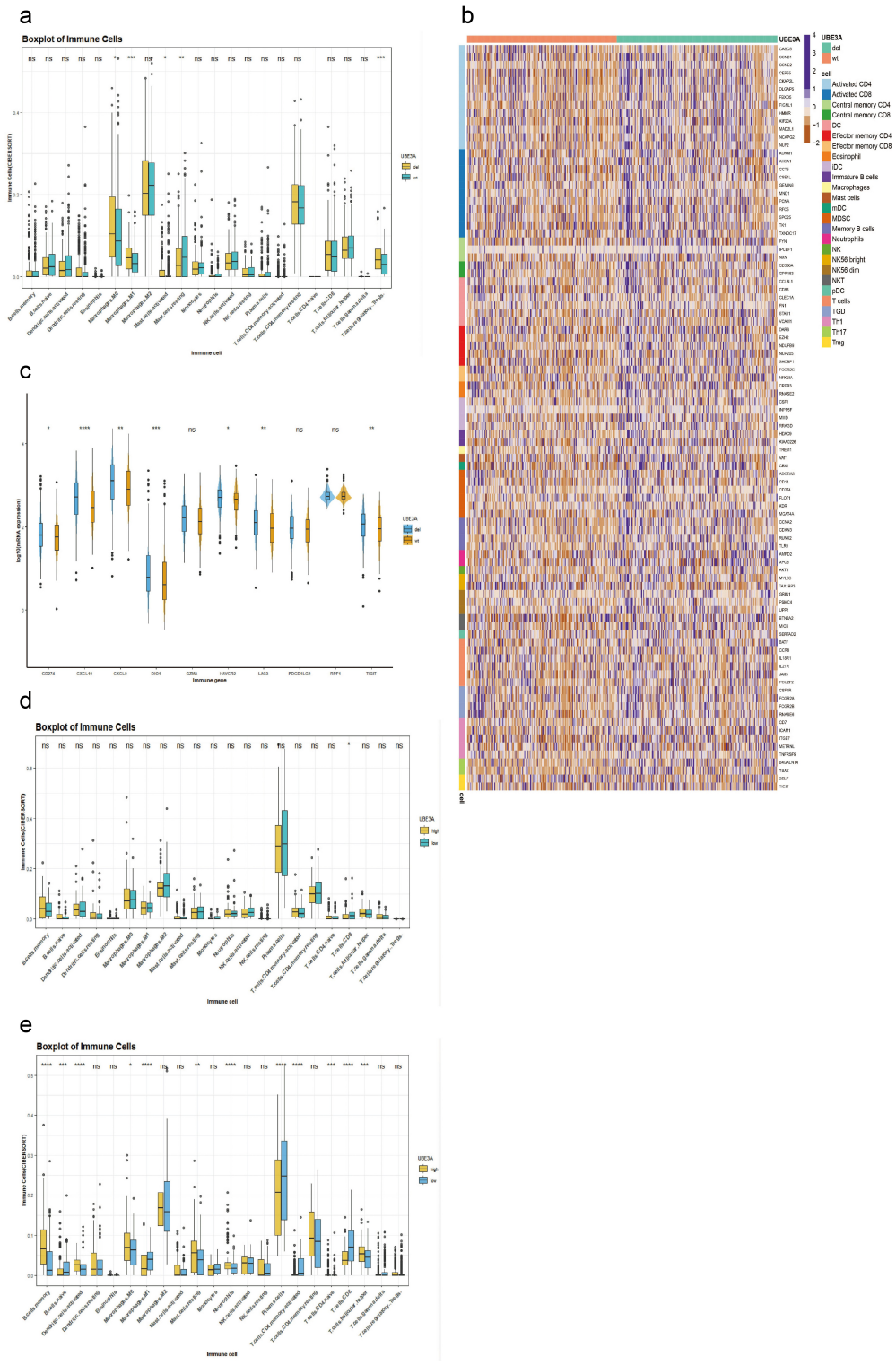


Figure 5. Relationship between *UBE3A*-del and *UBE3A*-wt in immune-infiltrating cell level and immune gene. (a) CIBERSORTx results of the TCGA-NSCLC dataset were based on the differences in the infiltration abundance of 22 kinds of immunocytes with *UBE3A* deletion. (b) Differential expression of immune genes in the TCGA-NSCLC cohort according to *UBE3A*-del and *UBE3A*-wt. Each line represents the expression of one gene. (c) Differential expression of important immune biomarkers, between *UBE3A*-del and *UBE3A*-wt in the TCGA-NSCLC dataset. (d) The results of CIBERSORT analysis of the GSE43580 cohort were analyzed according to the difference in the infiltration abundance of 22 kinds of immunocytes with *UBE3A* deletion. (e) The results of CIBERSORTx of the GSE63074 dataset were analyzed according to the difference in the infiltration abundance of 22 kinds of immunocytes with *UBE3A* deletion.

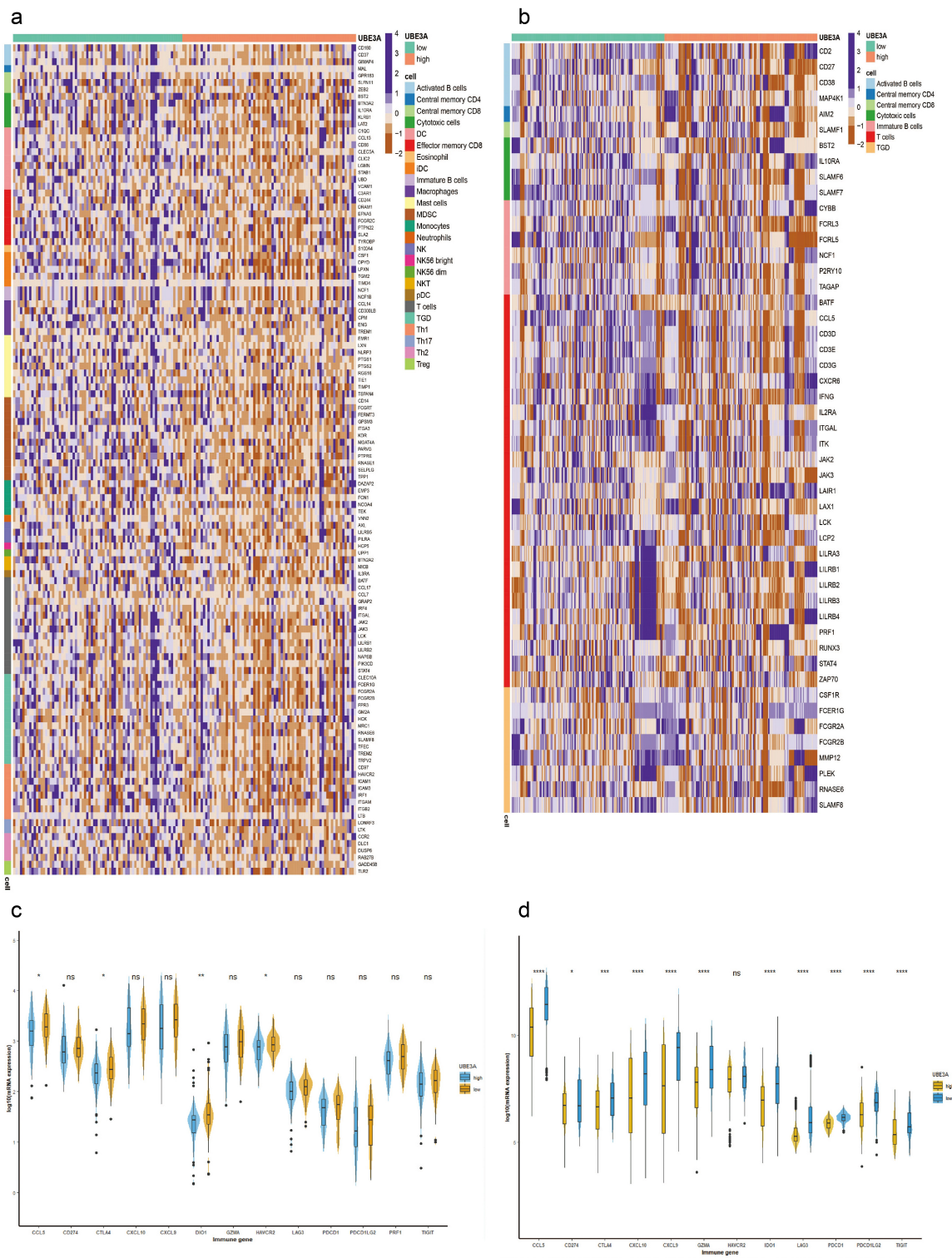


Figure 6. Relationship between *UBE3A-del* and *UBE3A-wt* in immune gene and immune biomarker. (a) Differential expression of immune genes in the GSE43580 dataset according to *UBE3A-del* and *UBE3A-wt*. Each line represents the expression of one gene. (b) Differential expression of immune genes in the GSE63074 dataset according to *UBE3A-del* and *UBE3A-wt*. Each line represents the expression of one gene. (c) Differential expression of important immune genes, between *UBE3A-del* and *UBE3A-wt* in the GSE43580 cohort. (d) Differential expression of important immune genes, between *UBE3A-del* and *UBE3A-wt* in the GSE63074 cohort.

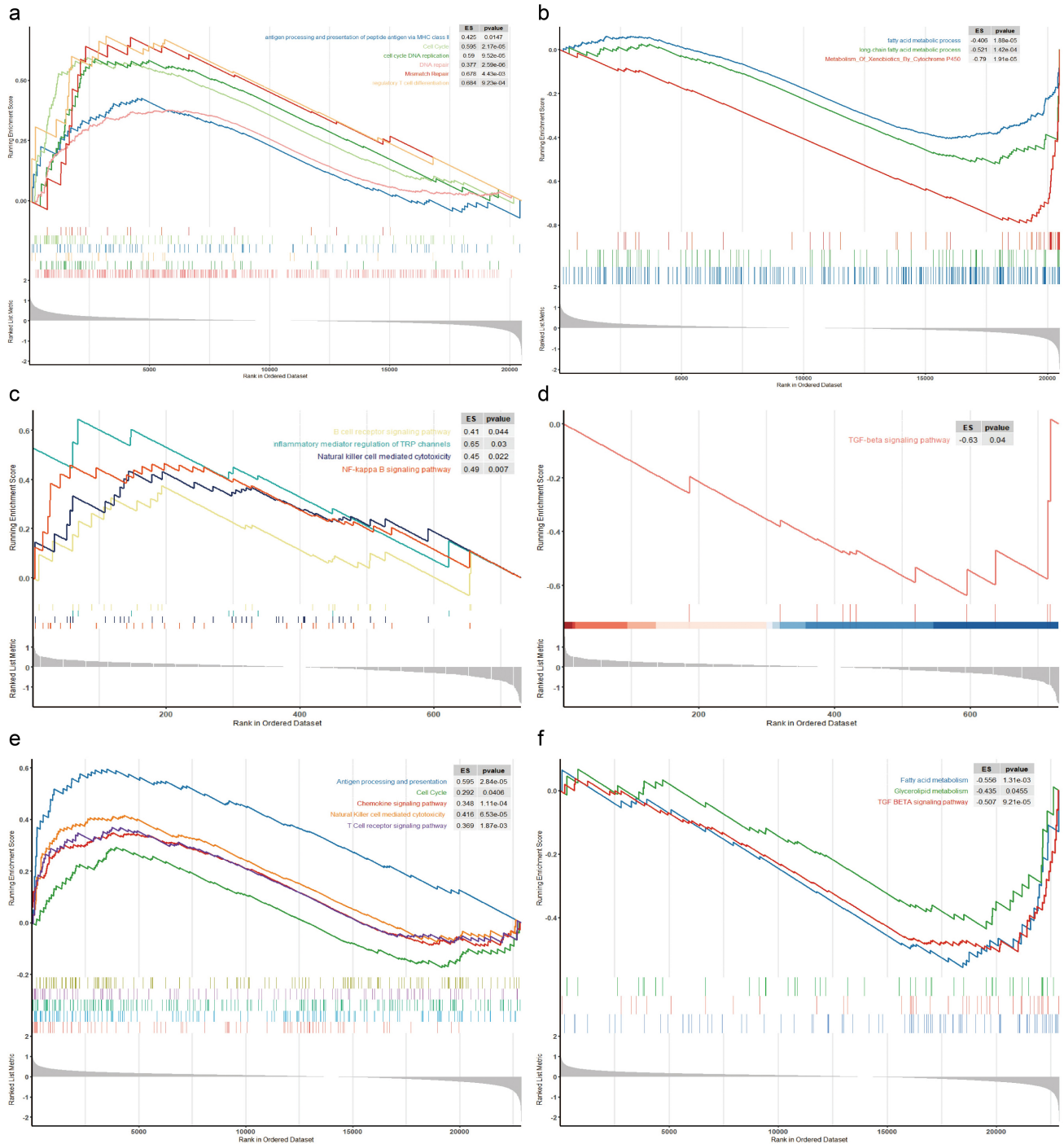


Figure 7. Effect of *UBE3A*-del on the influence of pathways(GSEA). (a) The results of GSEA of the TCGA-NSCLC cohort showed activated pathway in *UBE3A*-del and *UBE3A*-wt pathway enrichment, with p value of 0.05 representing a significant difference. (b) The results of GSEA of the TCGA-NSCLC cohort suggested inhibited pathway in *UBE3A*-del and *UBE3A*-wt pathway enrichment. (c) The results of GSEA of the GSE43580 cohort showed activated pathway in *UBE3A*-low and *UBE3A*-high pathway enrichment, with p value of 0.05 representing a significant difference. The results of GSEA of the GSE43580 cohort showed inhibited pathway in *UBE3A*-low and *UBE3A*-high pathway enrichment. (d) The results of GSEA of the GSE63074 cohort showed activated pathway in *UBE3A*-low and *UBE3A*-high pathway enrichment, with p value of 0.05 representing a significant difference. (e) The results of GSEA of the GSE63074 cohort showed inhibited pathway in *UBE3A*-low and *UBE3A*-high pathway enrichment.

CXCL9, and *CXCL10*) and immune checkpoint markers (*CTLA4*, *DIO1*, *HAVCR2*, and *PDCD1*) was significantly upregulated in *UBE3A*-low cells ($P < 0.05$, Figure 6(c,d)). In conclusion, our results show that *UBE3A*-del enhances antitumour immunity and immunogenicity.

***UBE3A*-del is enriched in the immune pathway**

We used the clusterProfiler package to explore the effect of *UBE3A*-del on pathways. Analysis results showed that *UBE3A*-del activated the DNA damage repair mismatch complex pathway. Previous studies have found that DNA damage and DDR gene changes could improve the efficacy of ICIs [35–37]. Activation of the MHC-II pathway enhanced the immune induction of CD4+ lymphocytes (Figure 7(a)). We also found that the downregulation of metabolism-related pathways relieved their immunosuppressive effect [38] (Figure 7(b)). GSEA of the GSE43580 and GSE63074 GEO datasets also showed that *UBE3A*-low activated immune pathways, such as B cell receptors, T cell receptors, antigen presentation, NK cells, cytokines and the cell cycle. In addition, metabolism-related pathways were inhibited after *UBE3A*-del in the TCGA cohort, and fatty acid metabolism-related pathways and TGF- β pathways were inhibited in the *UBE3A*-low GEO cohort (Figure 7(c-f)).

To deeply explore the influence of *UBE3A*-del on pathways, we analyzed ssGSEA on the TCGA-NSCLC dataset and GEO dataset. The TCGA analysis results showed that *UBE3A*-del had a significant effect on the activation level of the pathway. The upregulation of autophagy, the cell cycle, B cells, T cells, DNA damage repair, *TP53* and other pathways was significantly higher in *UBE3A*-del than in *UBE3A*-wt ($P < 0.05$, Figure 8(a)). These pathways had a positive regulatory effect on antitumour immunity. Analysis of the GEO cohort showed that *UBE3A*-low was enriched in the DNA damage repair, cell cycle, antigen presentation and *TP53* pathways, while fatty acid metabolism and TGF- β were inhibited ($P < 0.05$, Figure 8(b, c)). These results show that *UBE3A*-del increases

the effect of immunotherapy by upregulating the immune pathway.

Discussion

In this study, we gathered NSCLC datasets, including MSKCC, TCGA and GEO datasets. We selected genes relevant to CNV and prognosis from the MSKCC cohort based on ICI therapy and corresponding clinical data. Finally, we found that *UBE3A*-del was more relevant to ICIs. *UBE3A*-del was clustered in patients who responded to immunotherapy, which could predict the benefits of patients with *UBE3A*-del.

Although a growing number of studies have demonstrated that chromosome CNV is relevant to ICIs [18,19], there is a deficiency in the accurate relationship between genome changes in CNV and the efficacy of immunotherapy. Romualdo Barroso Sousa et al. found that *PTEN* deletion was reelevated by decreasing tumor immunocyte infiltration and reducing the reaction to immune checkpoint inhibitors [18]. Yuchen et al. suggested that *CCND1* amplification might inhibit the tumor microenvironment (TME) and hinder the immune response of natural hosts, thus affecting the efficacy of ICIs [19]. Our study found that *UBE3A*-del patients had higher TMB and longer PFS related to immunotherapy, and the CNV of *UBE3A* was positively correlated with mRNA expression and negatively correlated with methylation degree, which was consistent with previous research results [26,27,39]. Thijs Stutvoet et al. found that the MAPK pathway was important in inducing PD-L1 expression in lung cancer and might be a potential target for immune checkpoint inhibitors [32]. Hassan Wael et al. revealed that Notch1 could control cell proliferation and apoptosis [33]. In our study, the expression of these proteins in *UBE3A*-del exceeded that in *UBE3A*-wt.

We analyzed the common driver genes of NSCLC and discovered that the mRNA expression of *BRAF*, *KRAS*, and *MET* was higher after *UBE3A*-del. J Mazieres et al. reported a multicentre study on immunotherapy in 551 NSCLC patients in 2019. The study found that the *KRAS* gene-driven lung cancer ICI treatment response rate was the highest at 26%, followed by *BRAF*, with a response rate of 24%, and the *MET*-

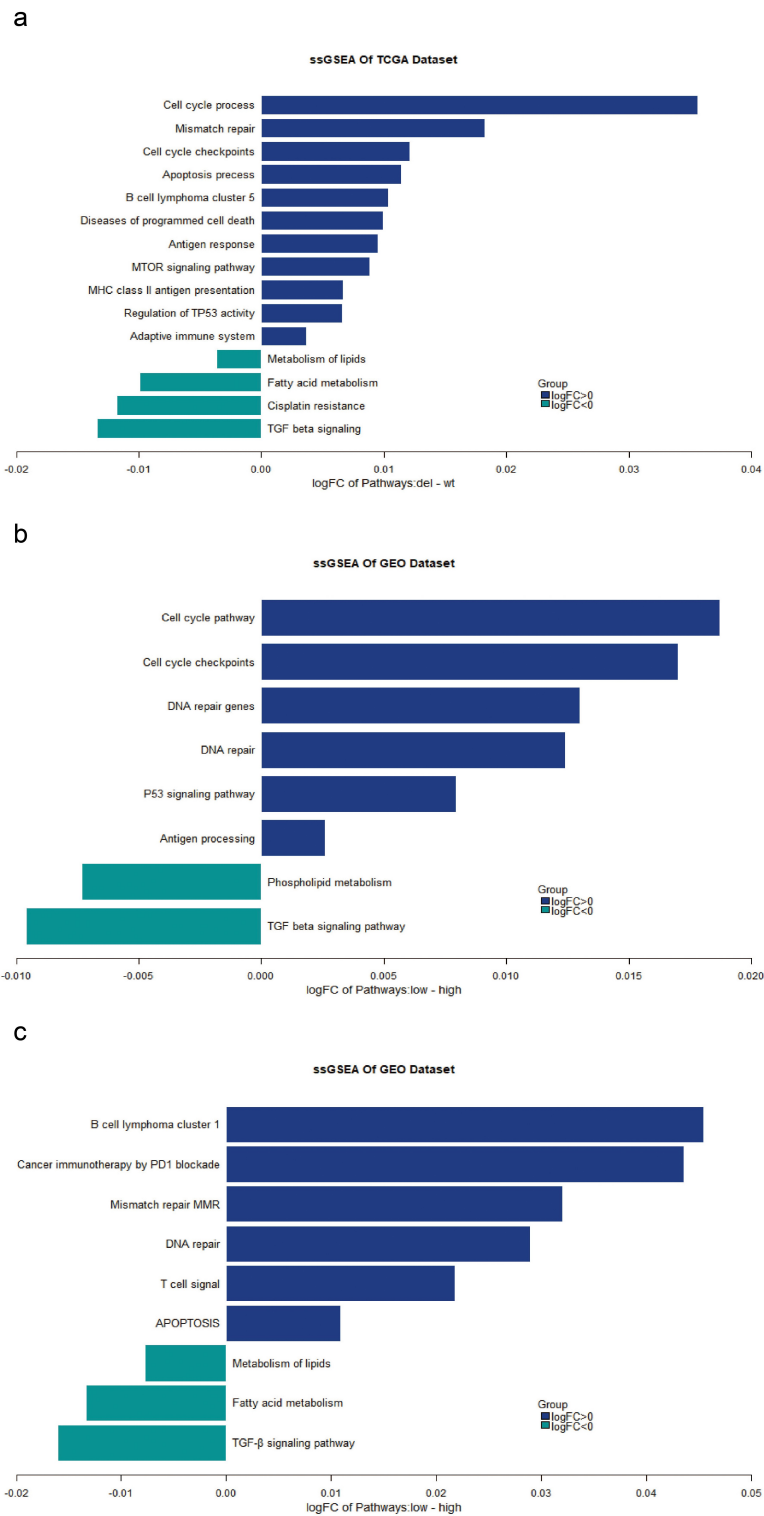


Figure 8. Effect of *UBE3A*-del on the influence of pathways(ssGSEA). (a) TCGA-NSCLC cohort ssGSEA analysis based on *UBE3A*-del and *UBE3A*-wt for the difference in the degree of pathway enrichment. (b) GSE43580 cohort ssGSEA analysis based on *UBE3A*-low and *UBE3A*-high for the difference in the degree of pathway enrichment. (c) GSE63074 cohort ssGSEA analysis based on *UBE3A*-low and *UBE3A*-high for the difference in the degree of pathway enrichment.

driven lung cancer ICI response rate was 16%, which were relatively higher than those of other driver genes [30]. In addition, *UBE3A*-del was

highly infiltrated in immunocytes, highly expressed immune genes, and affected immune-, autophagy-, and DNA damage repairable

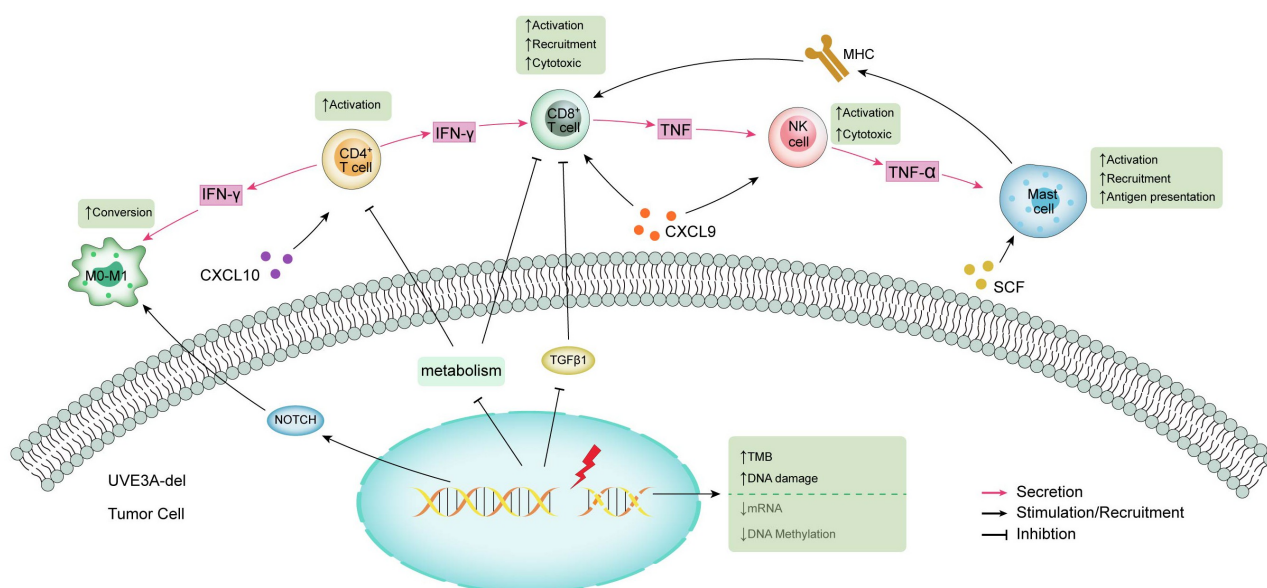


Figure 9. The possible mechanism of improving the prognosis of *UBE3A*-del NSCLC with ICIs.

pathways. These sequencing data analyzed based on various databases increased the evidence of the close relationship between *UBE3A*-del and NSCLC ICI efficacy, which supported epigenetics and immunotherapy.

This is the first report of CNV alteration *UBE3A*-del, which is closely related to NSCLC immunotherapy. *UBE3A* is also known as ubiquitin protein ligase E3A. The ubiquitin proteasome pathway participates in the regulation of the cell cycle, which is the principal protein degradation pathway, signal transduction and DNA damage repair. We summarized the possible mechanism of *UBE3A* in the treatment of ICIs (Figure 9). The deletion of *UBE3A* leads to gene changes, increased tumor mutation load, aggravated DNA damage, decreased mRNA expression and DNA methylation, thus activating immune-related pathways and consistent metabolism and the TGF- β pathway, which relieves the inhibition of CD4 and CD8 T cells and activates macrophages to activate the body's response to immunotherapy. Our study revealed that *UBE3A*-del was a potential biomarker of ICIs for NSCLC [40–42].

Previous prediction methods based on markers, including PD-L1 and TMB, are inaccurate, and their shortcomings were not sufficiently accurate. For example, in advanced non-small-cell lung cancer, the PD-L1 detection methods, interpretation criteria, and

cutoff values of different immunotherapy drugs are different. Immunotherapy may not be effective for patients with high expression of PD-L1 [43], while it may not be completely ineffective for patients with low PD-L1 expression [44]. Although most studies sustain the high forecast value of TMB [45,46], the detection methods of TMB are distinct, lacking accurate synonymous methods and cutoff values. Therefore, the test of a gene alteration to guide immunotherapy was more accurate, and we could easily obtain the genome change results of patients through sequencing results.

Previous studies have revealed that the Th1 chemokines *CXCL9* and *CXCL10* enhance the tumor attack of effector T cells and increase PD-L1 blockade [47]. Min Yuen Teo et al. found that changes in DDR genes were related to increases in TMB and improvements in clinical prognosis [40,41]. N Auphan et al. suggested that the NF- κ B signaling pathway activated cellular immunity by activating immune-related genes [48]. Previous research suggested that TGF- β could form the TME by limiting T cell infiltration, thus inhibiting antitumour immunity [49]. In our study, TGF- β pathways were inhibited in the *UBE3A*-low GEO cohort. In addition, Fokhrul Hossain et al. found that the energy metabolism pathway played an important role in the differentiation and function of immune cells. Myeloid-derived suppressor cells (MDSCs) promote

tumor growth by increasing fatty acid uptake and activating fatty acid oxidation (FAO) to inhibit T cell immunity, thus promoting the proliferation and migration of malignant cells. The inhibition of FAO alone could significantly delay the growth of T cell-dependent tumors and increase adoptive T cells and the antitumour effect of treatment [38]. Mauro Di Pilato et al. suggested that a few Treg cells were sufficient to produce this antitumour effect. This result showed that the activation of Treg cells was not enough to fully inhibit the immune system (Figure 5(a)). On the other hand, we might not have enough samples, which led to Treg cells being activated simultaneously with macrophages and mast cells [50]. In our study, *UBE3A*-del resulted in the upregulation of the chemokines *CXCL9* and *CXCL10*, the enrichment of the DDR pathway and the inhibition of the metabolic pathway, which were consistent with the findings of previous reports.

Although *UBE3A*-del has significant predictive value for NSCLC, the limitation of this study is that we only used bioinformatics to analyze the predictive value of *UBE3A*-del in only the immunotherapy of NSCLC, which is unknown for other tumors, and lacked verification in experiments and clinics. Further validation results are still needed to verify the predictive value of *UBE3A*-del in the immunotherapy of NSCLC, and it is necessary to expand to other tumors to further analyze its predictive value for immunotherapy.

Conclusion

Our study provides solid evidence that *UBE3A*-del patients have better PFS with ICIs. Consequently, *UBE3A*-del can be used as a new marker for the ICIs of NSCLC. We still need to verify this result in the clinic and expand the predicted tumor range in clinical practice.

Author contributions

Devised:NZ,PL;calculation and visualization:JS,LYG,NZ;control:PL, JZ; writing and translation:MMC,WMD.All authors participated in the study and approved the submission.

Disclosure statement

No potential conflict of interest was reported by the author(s).

Funding

This work was supported by a grant from the Luoyang science and technology development plan project (2101057A) and grants from Joint construction project of Henan Medical Science and technology research plan (LHGJ20200854).funding associated with the work featured in this article

ORCID

Jian Zhang  <http://orcid.org/0000-0001-7217-0111>

References

- [1] Chen DS, Mellman I. Elements of cancer immunity and the cancer-immune set point. *Nature*. 2017;541:321–330.
- [2] Sharma P, Huleskovan S, Wargo JA, et al. Primary, adaptive, and acquired resistance to cancer immunotherapy. *Cell*. 2017;168(4):707.
- [3] Somasundaram A, Socinski MA, Villaruz LC. Immune checkpoint blockade in lung cancer. *Discov Med*. 2016 Aug;22(119):55–65.
- [4] Remon J, Hendriks LE, Cabrera C, et al. Immunotherapy for oncogenic-driven advanced non-small cell lung cancers: is the time ripe for a change? *Cancer Treat Rev*. 2018 Dec;71:47–58.
- [5] Havel JJ, Chowell D, Chan TA. The evolving landscape of biomarkers for checkpoint inhibitor immunotherapy. *Nat Rev Cancer*. 2019;19(3):133–150.
- [6] Duruisseaux M, Martinez-Cardus A, Calleja-Cervantes ME, et al. Epigenetic prediction of response to anti-PD-1 treatment in non-small-cell lung cancer: a multicentre, retrospective analysis. *Lancet Respir Med*. 2018;6(10):771–781.
- [7] Ott PA, Bang YJ, Piha-Paul SA, et al. T-cell-inflamed gene-expression profile, programmed death ligand 1 expression, and tumor mutational burden predict efficacy in patients treated with Pembrolizumab across 20 cancers: KEYNOTE-028. *J Clin Oncol*. 2019;37(4):318–327.
- [8] Samstein RM, Lee CH, Shoushtari AN. Tumor mutational load predicts survival after immunotherapy across multiple cancer types. *Nat Genet*. 2019;51(2):202–206.
- [9] Chang L, Chang M, Chang HM, et al. Microsatellite instability: a predictive biomarker for cancer immunotherapy. *Appl Immunohistochem Mol Morphol*. 2018 Feb;26(2):e15–e21.
- [10] Le DT, Durham JN, Smith KN, et al. Mismatch repair deficiency predicts response of solid tumors to PD-1 blockade. *Science*. 2017 [Jul 28];357(6349):409–413.
- [11] Gasser S, Lina HK, Lim F, et al. The role of the tumour microenvironment in immunotherapy. *Endocr Relat Cancer*. 2017 Dec;24(12):T283–T295.
- [12] RobertDSchreiber T, Schreiber RD. Neoantigens in cancer immunotherapy. *Science*. 2015 [Apr 3];348(6230):69–74.

- [13] Zhang Y, Zhu Y, Wang J, et al. A comprehensive model based on temporal dynamics of peripheral T cell repertoire for predicting post-treatment distant metastasis of nasopharyngeal carcinoma. *Cancer Immunol Immunother.* 2021 [Aug 3];71(3):675–688.
- [14] Hao-Xiang W, Chen Y-X, Wang Z-X, et al. Alteration in TET1 as potential biomarker for immune checkpoint blockade in multiple cancers. *J Immunother Cancer.* 2019 [Oct 17];7(1):264.
- [15] Niu Y, Lin A, Luo P, et al. Prognosis of lung adenocarcinoma patients with NTRK3 mutations to immune checkpoint inhibitors. *Front Pharmacol.* 2020 [Aug 12];11:1213.
- [16] Zhang J, Zhou N, Lin A, et al. ZFH3 mutation as a protective biomarker for immune checkpoint blockade in non-small cell lung cancer. *Cancer Immunol Immunother.* 2020 [Jul 11];70(1):137–151.
- [17] Ruibin Y, Anqi L, Manming C, et al. ATM mutations benefit bladder cancer patients treated with immune checkpoint inhibitors by acting on the tumor immune. *Micro Front Genet.* 2020 [Aug 14];11:933.
- [18] Barroso-Sousa R, Keenan TE, Pernas S, et al. Tumor mutational burden and pten alterations as molecular correlates of response to PD-1/L1 blockade in metastatic triple-negative breast cancer. *Clin Cancer Res.* 2020 [Jun 1];26(11):2565–2572.
- [19] Davoli T, Uno H, Wooten EC, et al. Tumor aneuploidy correlates with markers of immune evasion and with reduced response to immunotherapy. *Science.* 2017 [Jan 20];355(6322):eaaf8399.
- [20] Cheng DT, Mitchell TN, Zehir A, et al. Memorial Sloan Kettering-integrated mutation profiling of actionable cancer targets (MSK-IMPACT): a hybridization capture-based next-generation sequencing Clinical assay for solid tumor molecular oncology. *J Mol Diagn.* 2015 May;17(3):251–264.
- [21] Gao J, Aksoy BA, Dogrusoz U, et al. Integrative analysis of complex cancer genomics and clinical profiles using the cBioPortal. *Sci Signal.* 2013;6(269):11.
- [22] Craig HM, Steven ES, Hill B, et al. Gad Getz. GISTIC2.0 facilitates sensitive and confident localization of the targets of focal somatic copy-number alteration in human cancers. *Genome Biol.* 2011;12(4):R41.
- [23] Mayakonda A, Lin DC, Assenov Y, et al. Maftools: efficient and comprehensive analysis of somatic variants in cancer. *Genome Res.* 2018;28(11):1747–1756.
- [24] Chen B, Khodadoust MS, Long Liu C, et al. Profiling tumor infiltrating immune cells with CIBERSORT. *Methods Mol Biol.* 2018;1711:243–259.
- [25] Yu G, Wang LG, Han Y, et al. clusterProfiler: an R package for comparing biological themes among gene clusters. *OMICS.* 2012;16(5):284–287.
- [26] S A, P T, Vk M, et al. Gene set enrichment analysis: a knowledge-based approach for interpreting genome-wide expression profiles[J]. *Proceedings of the National Academy of Sciences of the United States of America,* 2005, 102 (43):15545–15550. *Methods:Pathway enrichment analysis.*
- [27] Ritchie ME, Phipson B, Di W, et al. Limma powers differential expression analyses for RNA-sequencing and microarray studies. *Nucleic Acids Res.* 2015 [Apr 20];43(7):e47.
- [28] Hira R, Konnor La, et al. Molecular Determinants of Response to Anti-Programmed Cell Death (PD)-1 and Anti-Programmed Death-Ligand 1 (PD-L1) Blockade in Patients with Non-Small-Cell Lung Cancer Profiled with Targeted Next-Generation Sequencing. *J Clin .* 2018 Mar 1;36(7):633–641.
- [29] Kwon Y, Park S-J, Thanh Nguyen B, et al. Multi-layered proteogenomic analysis unravels cancer metastasis directed by MMP-2 and focal adhesion kinase signaling. *Sci Rep.* 2021 [Aug 24];11(1):17130.
- [30] Mazieres J, Drilon A, Lusque A, et al. Immune checkpoint inhibitors for patients with advanced lung cancer and oncogenic driver alterations: results from the IMMUNOTARGET registry. *Ann Oncol.* 2019 [Aug 1];30(8):1321–1328.
- [31] Jung H, Sook Kim H, Kim JY, et al. DNA methylation loss promotes immune evasion of tumours with high mutation and copy number load. *Nat Communications.* 2019 [Sep 19];10(1):4278.
- [32] Stutvoet TS, Kol A, Elisabeth Ge de V, et al. MAPK pathway activity plays a key role in PD-L1 expression of lung adenocarcinoma cells. *J Pathol.* 2019 Sep;249(1):52–64.
- [33] Hassan W, Ryoji Y, Shinji K, et al. Notch1 signaling controls cell proliferation, apoptosis and differentiation in lung carcinoma. *Lung Cancer.* 2014 Aug;85(2):131–140.
- [34] Yueming Z, Anqi L, Yonghe L, et al. Age and mutations as predictors of the response to immunotherapy in head and neck squamous cell cancer. *Front Cell Dev Biol.* 2020 [Dec 9];8:608969.
- [35] Teo MY, Seier K, Ostrovskaya, et al. Alterations in DNA damage response and repair genes as potential marker of clinical benefit from PD-1/PD-L1 blockade in advanced urothelial cancers. *J Clin Oncol.* 2018 [Jun 10];36(17):1685–1694.
- [36] Wang J, Wang Z, Zhao J, et al. Co-mutations in DNA damage response pathways serve as potential biomarkers for immune checkpoint blockade. *Cancer Res.* 2018 [Nov 15];78(22):6486–6496.
- [37] Wang S, Zou Z, Luo X, et al. LRH1 enhances cell resistance to chemotherapy by transcriptionally activating MDC1 expression and attenuating DNA damage in human breast cancer. *Oncogene.* 2018 Jun;37(24):3243–3259.
- [38] Hossain F, Al-Khamsi AA, Wyczechowska D, et al. Inhibition of fatty acid oxidation modulates immunosuppressive functions of myeloid-derived suppressor cells and enhances cancer therapies. *Cancer Immunol Res.* 2015 Nov;3(11):1236–1247.
- [39] Demidov G, Ossowski S. ClinCNV: novel method for allele-specific somatic copy-number alterations detection. *bioRxiv.* 2019.
- [40] Sun J, Liu Y, Jia Y, et al. UBE3A-mediated p18/LAMTOR1 Ubiquitination and Degradation regulate mTORC1 activity and synaptic plasticity. *Elife.* 2018 [Jul 18];7:e37993.

- [41] Martínez-Noël G, Luck K, Kühnle S, et al. Network analysis of UBE3A/E6AP-associated proteins provides connections to several distinct cellular processes. *J Mol Biol.* **2018** [Mar 30];430(7):1024–1050.
- [42] Yi JJ, Paranjape SR, Walker MP, et al. The autism-linked UBE3A T485A mutant E3 ubiquitin ligase activates the Wnt/ β -catenin pathway by inhibiting the proteasome. *J Biol Chem.* **2017** [Jul 28];292(30):12503–12515.
- [43] Honrubia-Peris B, Garde-Noguera J, García-Sánchez J, et al. Soluble biomarkers with prognostic and predictive value in advanced non-small cell lung cancer treated with immunotherapy. *Cancers (Basel).* **2021**;13(17):4280.
- [44] Patel SP, Kurzrock R. PD-L1 expression as a predictive biomarkers in cancer immunotherapy. *Mol Cancer Ther.* **2015** Apr;14(4):847–856.
- [45] Cristescu R, Mogg R, Ayers M, et al. Pan-tumor genomic biomarkers for PD-1 checkpoint blockade-based immunotherapy. *Science.* **2019** [Mar 1];363(6430):eaax 1384.
- [46] Ozaki Y, Muto S, Takagi H, et al. Tumor mutation burden and immunological, genomic, and clinicopathological factors as biomarkers for checkpoint inhibitor treatment of patients with non-small-cell lung cancer. *Cancer Immunol Immunother.* **2020** Jan;69(1):127–134.
- [47] Peng D, Kryczek I, Nagarsheth N, et al. Epigenetic silencing of TH1-type chemokines shapes tumour immunity and immunotherapy. *Nature.* **2015** [Nov 12];527(7577):249–253.
- [48] Auphan N, DiDonato JA, Rosette C, et al. Immunosuppression by glucocorticoids: inhibition of NF-kappa B activity through induction of I kappa B synthesis. *Science.* **1995** [Oct 13];270(5234):286–290.
- [49] Mariathasan S, Turley SJ, Nickles D, et al. TGF β Attenuates tumour response to PD-L1 blockade by contributing to exclusion of T cells. *Nature.* **2018** [Feb 22];554(7693):544–548.
- [50] Di M, Pilato EY, Bruno K, et al. Targeting the CBM complex causes T reg cells to prime tumours for immune checkpoint therapy. *Nature.* **2019** Jun;570(7759):112–116.